Article

Cell Host & Microbe

Bacteriostatic antibiotics promote CRISPR-Cas adaptive immunity by enabling increased spacer acquisition

Graphical abstract

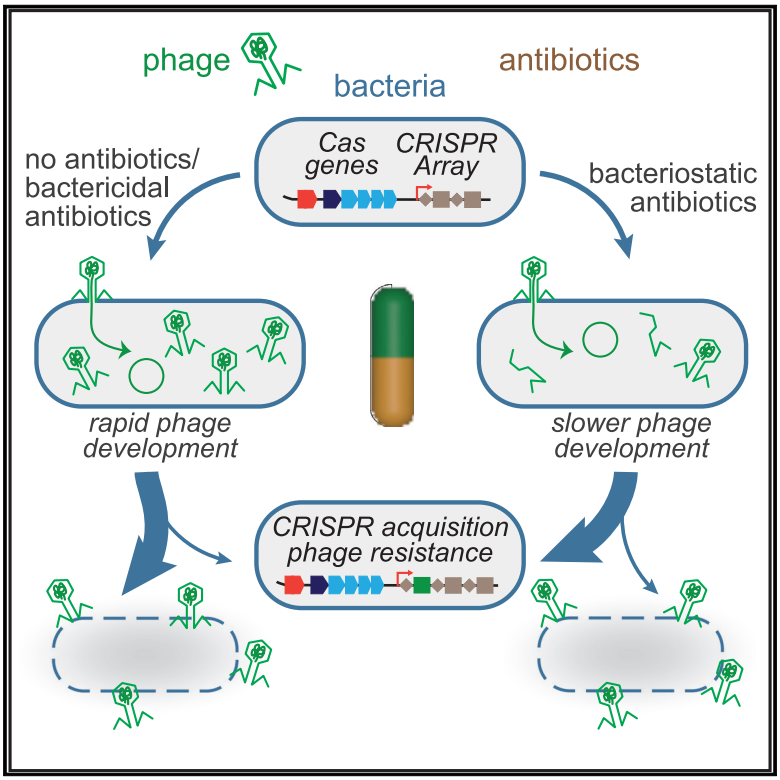

Highlights

- Bacteriostatic antibiotics promote evolution of CRISPR-Cas immunity against phages
- Bacteriostatic antibiotics slow down phage replication
- Slower phage development allows more time for cells to acquire spacers
- Other environmental factors slowing down cell growth also promote CRISPR-Cas immunity

Authors

Tatiana Dimitriu, Elena Kurilovich, Urszula Łapińska, Konstantin Severinov, Stefano Pagliara, Mark D. Szczelkun, Edze R. Westra

Correspondence

t.dimitriu@exeter.ac.uk (T.D.), e.r.westra@exeter.ac.uk (E.R.W.)

In brief

Dimitriu et al. find that bacteriostatic antibiotics, which inhibit bacterial cell growth without killing, promote CRISPR-Cas immunity by slowing down phage replication. Delayed production of mature phage particles allows more time for cells to acquire spacers against phages. Other environmental factors slowing down cell growth also promote CRISPR-Cas immunity.

Dimitriu et al., 2022, Cell Host & Microbe *30*, 31–40
January 12, 2022
https://doi.org/10.1016/j.chom.2021.11.014

CellPress

Cell Host & Microbe

CellPress
OPEN ACCESS

Article

Bacteriostatic antibiotics promote CRISPR-Cas adaptive immunity by enabling increased spacer acquisition

Tatiana Dimitriu,[1,8,*] Elena Kurilovich,[2] Urszula Łapińska,[3] Konstantin Severinov,[2,4,5,6] Stefano Pagliara,[3] Mark D. Szczelkun,[7] and Edze R. Westra[1,*]

[1]ESI, Biosciences, University of Exeter, TR10 9FE Penryn, UK
[2]Center of Life Sciences, Skolkovo Institute of Science and Technology, Moscow 143028, Russia
[3]Living Systems Institute and Biosciences, University of Exeter, EX4 4QD Exeter, UK
[4]Waksman Institute of Microbiology, Piscataway, NJ 08854, USA
[5]Institute of Molecular Genetics, Russian Academy of Sciences, Moscow 119334, Russia
[6]Center for Precision Genome Editing and Genetic Technologies for Biomedicine, Institute of Gene Biology, Russian Academy of Sciences, Moscow 119334, Russia
[7]DNA-Protein Interactions Unit, School of Biochemistry, University of Bristol, BS8 1TD Bristol, UK
[8]Lead contact
*Correspondence: t.dimitriu@exeter.ac.uk (T.D.), e.r.westra@exeter.ac.uk (E.R.W.)
https://doi.org/10.1016/j.chom.2021.11.014

SUMMARY

Phages impose strong selection on bacteria to evolve resistance against viral predation. Bacteria can rapidly evolve phage resistance via receptor mutation or using their CRISPR-Cas adaptive immune systems. Acquisition of CRISPR immunity relies on the insertion of a phage-derived sequence into CRISPR arrays in the bacterial genome. Using *Pseudomonas aeruginosa* and its phage DMS3vir as a model, we demonstrate that conditions that reduce bacterial growth rates, such as exposure to bacteriostatic antibiotics (which inhibit cell growth without killing), promote the evolution of CRISPR immunity. We demonstrate that this is due to slower phage development under these conditions, which provides more time for cells to acquire phage-derived sequences and mount an immune response. Our data reveal that the speed of phage development is a key determinant of the evolution of CRISPR immunity and suggest that use of bacteriostatic antibiotics can trigger elevated levels of CRISPR immunity in human-associated and natural environments.

INTRODUCTION

Bacterial populations are shaped by their coevolution with phages, viruses that infect bacteria (Chevallereau et al., 2021). In response to phage predation, bacteria have evolved a wide range of mechanisms that confer resistance (Hampton et al., 2020; Labrie et al., 2010). Approximately 40% of sequenced bacterial genomes encode CRISPR-Cas immune systems, which enable bacteria to rapidly acquire phage resistance by inserting phage-derived sequences (spacers) into CRISPR loci on the bacterial genome (Barrangou et al., 2007). Acquisition of spacers takes place during the course of a phage infection and is followed by transcription of the CRISPR array that contains the newly acquired spacer, processing of the CRISPR transcript to generate mature crRNAs and assembly of crRNA-Cas ribonucleoprotein effector complexes that detect phage genomes in the cell through complementary base pairing and eliminate them through nucleolytic cleavage (reviewed in Hampton et al. [2020]). The time it takes to carry out all these steps from spacer acquisition to phage DNA cleavage may constrain the ability of CRISPR-Cas immune systems to protect against rapidly replicating phages, since they all need to be completed before the cell is irrevocably damaged by the phage (Horvath and Barrangou, 2010). This issue was addressed in a seminal study on spacer acquisition by the type II-A CRISPR-Cas system of *Streptococcus thermophilus* strain DGCC7710, which revealed that virtually all spacer acquisition events from its lytic phage 2,972 resulted from defective phage particles that inject their genome into the bacterial cell but are unable to replicate (Hynes et al., 2014). This and other studies also revealed that the presence of a restriction-modification system increases the frequency of spacer acquisition events, not only because phage replication is prevented due to endonucleolytic cleavage of the unmethylated phage genome (Hynes et al., 2014) but also because free DNA ends are a substrate for spacer acquisition (Levy et al., 2015; Modell et al., 2017; Shiimori et al., 2017), reviewed in Dimitriu et al. (2020). Moreover, breakdown products that are subsequently generated through RecBCD or AddAB activity are thought to directly feed into the spacer acquisition machinery, which further promotes spacer acquisition (Levy et al., 2015; Modell et al., 2017). The link between DNA cleavage and degradation and subsequent spacer acquisition events also explains why pre-existing spacers that partially or fully match the genome of infecting phage lead to enhanced rates of spacer acquisition, a process known as priming (Datsenko et al., 2012; Fineran et al., 2014; Künne et al., 2016; Nussenzweig et al., 2019; Savitskaya

et al., 2013; Severinov et al., 2016; Staals et al., 2016; Swarts et al., 2012). From these studies a model has emerged where the rates of spacer acquisition are determined by both the frequency of defective phage particles in a population and the existence of mechanisms that introduce DNA breaks in the phage genome and that generate cleavage products that feed into the spacer acquisition machinery (reviewed in Jackson et al. [2017]).

One of the model organisms for studying the acquisition of CRISPR immunity is *Pseudomonas aeruginosa* strain PA14, which carries a type I-F CRISPR-Cas system containing a partially matching spacer against its phage DMS3vir (Cady et al., 2012), allowing primed spacer acquisition. *P. aeruginosa* PA14 rapidly evolves CRISPR immunity against this phage when cultured in nutrient-limited media (van Houte et al., 2016; Westra et al., 2015) but mostly evolves phage resistance through surface modification (SM) (loss or mutation of the type IV pilus, which is the DMS3vir receptor) in nutrient-rich broth and in artificial sputum medium that mimics the cystic fibrosis lung environment it commonly colonizes (Alseth et al., 2019; Westra et al., 2015). Unlike CRISPR immunity, mutation of the phage receptor leads to attenuated virulence (Alseth et al., 2019), and it is therefore key to predict and manipulate which mechanism bacteria use to become phage resistant under clinically relevant conditions.

P. aeruginosa is an important opportunistic human pathogen classified as a priority one pathogen by the World Health Organization. Infections are commonly treated with antibiotics, despite the emergence of multidrug-resistant strains that are selected during extended antibiotic treatment, for example, in the lungs of people with cystic fibrosis (Langendonk et al., 2021). Antibiotics can also affect the evolution of phage resistance (Torres-Barceló et al., 2018), for example, because bacterial mutation rates can be enhanced in response to antibiotics exposure (Baharoglu and Mazel, 2011; Kohanski et al., 2010), thus increasing the probability that they acquire mutations in phage receptor genes. Indeed, increases in *P. aeruginosa* mutation rates have been shown to result in higher levels of SM-based resistance and a corresponding decrease in the evolution of CRISPR immunity (Chevallereau et al., 2019). To understand the implications of antibiotics treatment on the evolution of CRISPR immunity in *P. aeruginosa*, we studied how eight different antibiotics influence the evolutionary dynamics of *P. aeruginosa* PA14 in response to phage DMS3vir. We show that bacteriostatic antibiotics promote the evolution of CRISPR immunity by delaying the production of mature phage particles, which allows more time for spacer acquisition during the course of a phage infection. We then generalize these findings to other conditions that slow down the speed of phage development. This work shows that, in addition to defective phages and nucleases that cleave phage genomes, the speed of phage development is a key determinant of the frequency of spacer acquisition by CRISPR-Cas immune systems.

RESULTS

Bacteriostatic antibiotics promote CRISPR immunity

To understand how antibiotics shape the population and evolutionary dynamics of *P. aeruginosa* during phage infection, we infected PA14 cultures grown in rich medium supplemented with sub-inhibitory concentrations of 8 different antibiotics (Table S1) with phage DMS3vir. Of these antibiotics, four are bactericidal (ciprofloxacin [Cip], streptomycin [Strep], gentamycin [Gen] and carbenicillin [Carb]) and four are bacteriostatic (chloramphenicol [Chl], tetracycline [Tc] erythromycin [Erm], and trimethoprim [Tm]) against *P. aeruginosa*. Of the bacteriostatic antibiotics, Chl and Tc had the strongest effects on bacterial exponential growth rate at the concentrations used, whereas Erm had little effect on exponential growth but instead slowed growth at a later stage, when bacteria reach high densities (Figure S1). Most antibiotics delayed the phage epidemics and subsequently the evolution of phage resistance (Figures S2A and S2B). Nonetheless, at 3 days post-infection (d.p.i.) phage resistance was essentially fixed in all cultures (Figure S2C). Strikingly, at this point, the type of phage resistance that had evolved was strongly dependent on the presence and the type of antibiotic. In the absence of antibiotics, or in the presence of bactericidal antibiotics, only a minority of bacteria evolved CRISPR immunity (Westra et al., 2015), whereas a large proportion of the bacterial population evolved CRISPR immunity in the presence of bacteriostatic antibiotics (Figures 1A and S2D). These data, and the fact that Chl, Tc, Erm, and Tm have different modes of action, suggest that bacteriostatic antibiotics promote evolution of CRISPR immunity because they limit bacterial growth rates.

To better understand the relationship between bacterial growth and evolution of CRISPR immunity, we first measured bacterial growth rates in the presence of each antibiotic at concentrations used in our evolution experiments. Analysis of exponential growth rates in batch culture (based on the optical density, OD600, of the cultures) and doubling times of individual cells in a microfluidics device showed that Chl and Tc cause particularly slow growth, and this is associated with a large increase in the evolution of CRISPR immunity (Figure 1B). More generally, this analysis revealed a correlation between exponential growth rate and the evolution of CRISPR immunity, with the exception of Erm (Pearson's correlation, $p = 0.11$ for exponential growth rate, $p = 0.26$ for doubling time when taking all antibiotics into account; $p = 0.008$, $\rho = -0.89$ for exponential growth rate and $p = 0.018$, $\rho = 0.89$ for doubling time when excluding Erm). Erm is known, similarly to other macrolides, to mostly affect bacterial growth and gene expression at high cell densities, instead of early exponential phase (Tateda et al., 2007) (consistent with our OD600 growth curves, in which growth is affected mostly after $\sim$10 h, and not measurable with our microfluidics setup). Moreover, in evolution experiments, phages undergo epidemic spread during the first 24 h, and the majority of phage infections occur after 12 h (Figure S2E). Thus, in the presence of all bacteriostatic antibiotics, most phage infection events will happen in cells experiencing reduced growth rates.

Bacteriostatic antibiotics promote spacer acquisition

We then asked whether the effect of bacteriostatic antibiotics on phage resistance evolution can be explained by a change in the rate of mutation toward SM or toward CRISPR immunity (by insertion of phage-derived spacers into CRISPR loci on the bacterial genome), or by affecting the fitness consequences of these alternative phage resistance mechanisms. To measure the effects of antibiotics on the frequency of spacer acquisition events leading to phage resistance, we performed short-term (3 h) infection

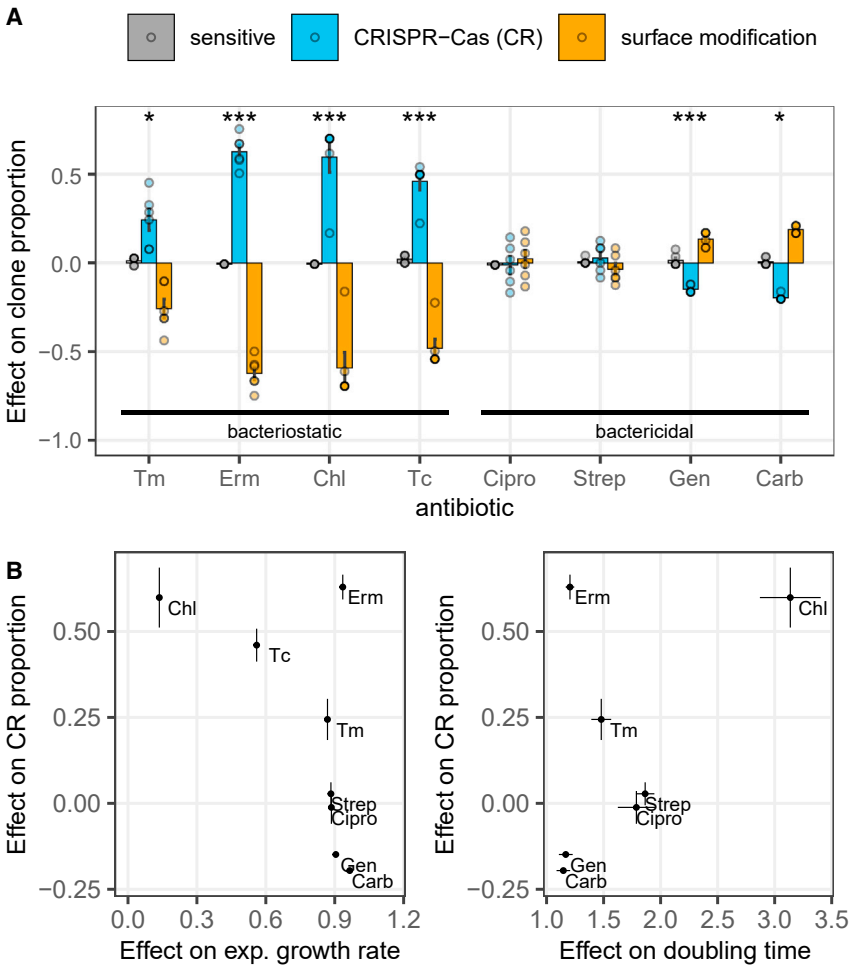

Figure 1. Bacteriostatic antibiotics promote CRISPR-Cas immunity

(A) Effect of each antibiotic on the proportion of sensitive (gray), CRISPR-Cas (blue) and SM clones (yellow) at 3 d.p.i., calculated as the change in proportion of each type of clone in the antibiotic treatment relative to the average proportion of this type of clone in the associated no-antibiotic treatment. Bars and error bars show mean ± SEM, and individual biological replicates are plotted as dots (n = 6). Asterisks indicate antibiotics with CRISPR-Cas proportion significantly different from the associated no-antibiotic treatment (*0.01 < p < 0.05; ***p < 0.001). Antibiotics are ordered from left to right by decreasing minimum bactericidal concentration/minimum inhibitory concentration ratio, a measure of their bacteriostatic versus bactericidal activity. Raw data are shown in Figure S2D.

(B) Antibiotic effect on 3 d.p.i. evolved CRISPR-Cas resistance (CR), shown as a function of antibiotic effect on exponential growth rate (measured by OD600 change in 96-well plates, left) and as a function of antibiotic effect on doubling time measured in microfluidics (right). Dots and error bars show mean ± SEM, respectively. See also Figures S1 and S2.

assays and measured the proportion of bacteria that had acquired CRISPR immunity in the presence or absence of each antibiotic. This limits the effect that natural selection has on the frequencies of CRISPR-immune bacteria in the population, which becomes increasingly important during longer-term experiments (Figure 1). Short-term infection experiments revealed that in the presence of all bacteriostatic antibiotics more cells acquired CRISPR immunity, whereas bactericidal antibiotics had no effect (Figure 2A). This effect was detectable despite bacteriostatic antibiotics inhibiting absolute cell growth (Figure S3). Across antibiotics, the frequency at which CRISPR immunity is acquired in these short-term experiments was significantly correlated to the levels of CRISPR immunity that evolved at 3 d.p.i. (Figure 2B, Pearson's correlation $t_{1,6} = 3.9$, $p = 0.008$, $\rho = 0.85$). In contrast, none of the antibiotics except Cip affected the rates at which bacteria with SM are generated (Figure S4A). Thus, all bacteriostatic antibiotics promoted acquisition of CRISPR immunity, while having no effect on SM resistance acquisition.

We next tested whether antibiotics impact the way selection acts on clones with CRISPR immunity and receptor mutants. Competition experiments between a clone with CRISPR immunity and a SM-resistant clone showed that the presence of bacteriostatic antibiotics had either no impact or reduced the fitness of CRISPR-immune bacteria relative to receptor mutants (Figure S4B). Therefore, the elevated frequencies of CRISPR immunity in the presence of bacteriostatic antibiotics cannot be explained by a selective advantage of CRISPR-immune bacteria over SM-resistant bacteria. Moreover, consistent with this conclusion, the bacteriostatic antibiotic Chl only triggered increased evolution of CRISPR immunity if it was present during the first day following phage infection (Figure S4C), when most cells are still phage sensitive (Figure S2C), and later exposure, when bacteria have already acquired resistance, had no effect. Collectively, these data show that the increase in the evolution of CRISPR immunity in the presence of bacteriostatic antibiotics can be explained by an increase in the frequency of spacer acquisition.

Bacteriostatic antibiotics slow down progeny phage production

The common feature of bacteriostatic antibiotics is that they inhibit cell growth, which might lead to higher rates of spacer acquisition (Høyland-Kroghsbo et al., 2018). Bacteriostatic and bactericidal antibiotics impact cell metabolism differently and lead, respectively, to decreased and increased cell metabolic rates (Lobritz et al., 2015). Because phage production is dependent on the metabolism and protein synthesis machinery of the host (Hadas et al., 1997; You et al., 2002), we hypothesized that bacteriostatic antibiotics may slow down phage development, providing a larger window of time for the CRISPR-Cas immune system to acquire spacers from the phage prior to irreversible cell damage or cell death. To test this hypothesis, we performed one-step phage growth assays to detect when mature intracellular phages are

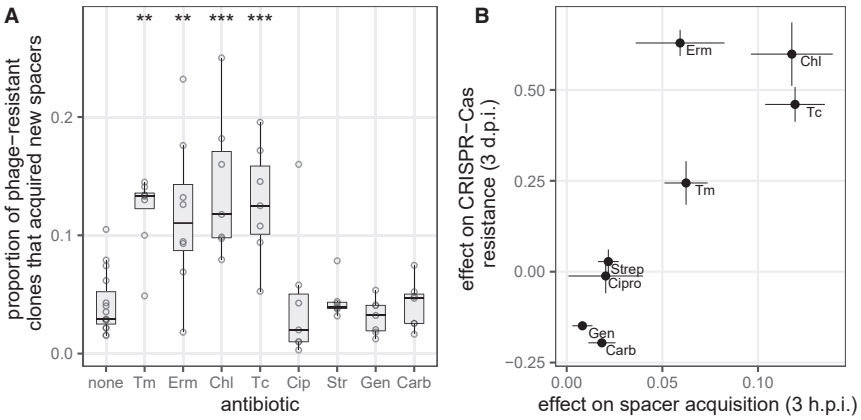

Figure 2. Bacteriostatic antibiotics increase acquisition of CRISPR immunity

(A) Proportion of resistant clones that are CRISPR-Cas immune after 3 h phage infection. The center value of the boxplots, boxes, and whiskers represent the median, respectively, first and third quartile, and 1.5 times the interquartile range; dots show individual data points (n= 6). Asterisks show treatments significantly different from the no-antibiotic control (Tukey HSD; **0.001 < p < 0.01; ***p < 0.001).

(B) Average change in proportion per treatment plotted against the average increase in proportion of CRISPR-Cas immune clones in the evolution experiments shown in Figure 1, error bars showing SEM (N = 6). See also Figure S3.

produced. First, we inoculated phages to cell cultures grown in each antibiotic treatment for 12 h (i.e., the time at which the majority of infections take place in our evolution experiments, see Figure S2E). We found that all bacteriostatic antibiotics caused a strong reduction in phage production compared with cells cultured in the absence of antibiotics (Figures 3A and S5). Under those conditions, we were unable to analyze the effect of bactericidal antibiotics on phage production, due to high rates of cell death in these treatments. To directly compare the effects of bacteriostatic and bactericidal antibiotics on phage progeny formation, we repeated these assays using a shorter period of antibiotics exposure (30 min, at which point bactericidal antibiotics do not affect viable cell density). Interestingly, we found that Erm had no effect on phage production (Figure 3B), consistent with its minor effect on exponential growth rate of the bacteria (Figure S1). All other bacteriostatic antibiotics (Chl, Tc, and Tm) delayed or impaired the formation of infectious progeny phages (Figure 3B). Bactericidal antibiotic had more variable effects: Cip and Carb showed no interference with the production of infectious phages, in agreement with their mechanism of action and known synergy with phage therapy (Comeau et al., 2007), whereas the presence of Strep or Gen (both aminoglycosides) resulted in very little phage production (Figure 3B). Finally, to understand whether some of these antibiotics might inhibit phage production altogether, we carried out highly replicated experiments (96 bacterial culture per treatment) of bacterial populations, each infected with a very small initial dose of phage (around 5 phage particles per infection experiment). After 24 h of infection, we measured how the proportion of successful phage amplification depends on the antibiotics present, hence providing an estimate of their impact on the probability of successful phage infection (Figure 3C). In the absence of antibiotics or in the presence of Tm, Chl, Cip and Carb, all infected populations ultimately produced new phages. However, phage amplification was abolished in almost all infection experiments in the presence of Gen, and in the majority of infection experiments in the presence of Strep. Thus, Strep and Gen ultimately inhibit phage production (Figure 3C) (Kever et al., 2021). Interestingly, we also observed a small but significant increase in failed infections in the presence of Erm and Tc. While this may contribute to the evolution of CRISPR immunity (Hynes et al., 2014), it is insufficient to explain the effects of bacteriostatic antibiotics in general, since these had only small (Erm and Tc) or no effects (Tm, Chl) on the proportion of unproductive infections (Figure 3C). With most infections being ultimately productive, the delayed production of infectious phage particles observed for all static antibiotics (Figure 3A) is thus due to a delay in the phage eclipse period.

In addition to delaying phage amplification, antibiotics may also cause DNA damage, creating free DNA ends that could increase spacer acquisition and thus promote the evolution of CRISPR immunity (Levy et al., 2015). To evaluate DNA damage, we quantified SOS response gene expression in the presence of each antibiotic (Figure S6A). We found that three antibiotics, Tc, Chl, and Cip, increased SOS gene expression levels. However, there was no correlation between SOS induction and the evolution of CRISPR immunity. Moreover, low concentrations of Chl, which still promote CRISPR immunity evolution (see Figure 4), led to almost no SOS induction (Figure S6A). Furthermore, treatment with mitomycin C at concentrations that induce the SOS response did not promote evolution of CRISPR immunity (Figure S6B). Therefore, these data do not support the hypothesis that DNA damage leads to increased frequencies of spacer acquisition in our model system.

Finally, we asked whether changes in Cas protein levels could contribute to acquisition of CRISPR immunity. None of the antibiotics caused an increase in Cas protein abundance (Figure S6C); thus, bacteriostatic antibiotic effect on the appearance of CRISPR-immune cells is not due to increased levels of the spacer acquisition machinery. Collectively, these data show that bacteriostatic antibiotics cause phage to replicate more slowly and increase the frequency at which initially sensitive cells acquire CRISPR immunity. We propose that there is a causal relationship between these two phenomena.

A wide range of Chl concentrations promotes CRISPR immunity

Until this point, we used one sub-MIC (minimum inhibitory concentration) for each antibiotic tested. During antibiotic treatment or in the environment, bacteria might be exposed to a much wider range of antibiotic concentrations. We therefore tested concentrations covering 0.05× to 3.3× MIC for the bacteriostatic antibiotic Chl, that resulted in a large range of effects on cell growth (Figure 4A). We found that Chl triggered CRISPR immunity across all concentrations tested, whereas no effect was

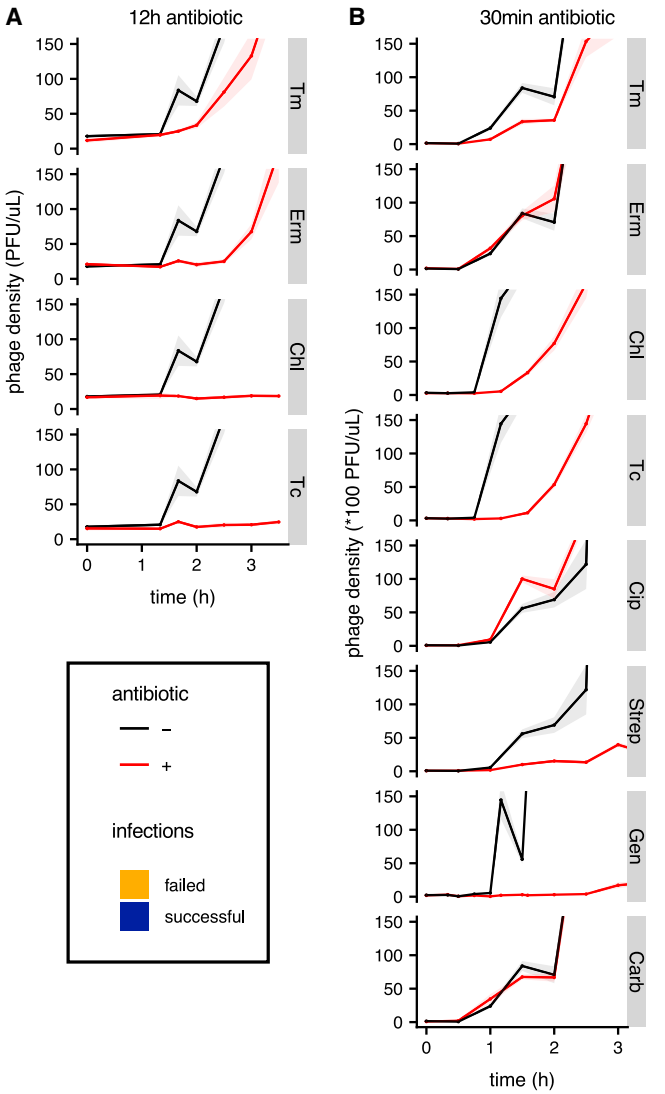

Figure 3. Bacteriostatic antibiotics delay production of mature phage particles

(A and B) Effect of antibiotics on phage production dynamics. Phage density over time during infection of cells that were pre-exposed to antibiotics for 12 h (A) or 30 min (B) are shown in red and no-antibiotic controls in black. The y axis is cropped to focus on antibiotic treatment dynamics, see Figure S5 for full dataset. Lines and shaded areas are, respectively, mean and SEM (n= 4).

(C) Effect of antibiotics on the frequency of failed phage infections. 96 parallel populations were infected with a low number of phages per population (~5) and grown for 24 h. Bar plots show the percentage of populations with failed infection (no phages detected after 24 h) or successful infection (infectious phages present after 24 h). Asterisks indicate antibiotics with a significant increase in the number of populations with no phages (chi-square tests, ***$p < 0.001$).

observed when we used a Chl-resistant strain (Figure 4B). Even a concentration as low as 0.05 MIC promoted CRISPR immunity evolution, despite minimally affecting the exponential growth rate. Nonetheless, even low Chl concentrations led to a reduction in growth at later time points (Figure 4A), and a corresponding large delay in phage production in infected cells (Figure 4C). Thus, bacteriostatic antibiotics can promote the acquisition of CRISPR immunity over a wide range of concentrations by affecting the phage development dynamics. By contrast, the bactericidal antibiotic Gen did not promote the emergence of CRISPR immunity in any of a wide range of concentrations tested (Figure S7).

Carbon sources associated with slow growth promote evolution of CRISPR immunity

Given that bacteriostatic antibiotics promote the evolution of CRISPR-immune bacteria, we hypothesized that other environmental factors that slow down cell growth could also lead to an increase in the evolution of CRISPR immunity by slowing down phage replication, as expected based on changes in cell metabolic rates (Payne et al., 2018; Rabinovitch et al., 2002; You et al., 2002). To test this hypothesis, we performed evolution experiments in minimal medium with different carbon sources. First, using eight different carbon sources, we measured whether bacterial growth rate varied across the different carbon sources. Measurement of OD600 showed that there was variation in bacterial growth rate across the different growth media (Figure 5A). Next, we explored whether there was variation in the levels of CRISPR immunity that evolved in response to phage across these same growth media. To this end, we infected bacterial cultures with phages and after co-culturing for 4 days, measured if and how bacteria had evolved phage resistance. This revealed variation in the levels of CRISPR immunity across growth media (Figure 5B, $F_{7,133} = 139$, $p < 2 \times 10^{-16}$). Growth on carbon sources associated with slower bacterial growth was correlated with increased CRISPR immunity (Figure 5C, Pearson correlation, $t_{1,6} = -2.68$, $p = 0.037$, $\rho = -0.74$), supporting our hypothesis that reductions in bacterial growth rate are associated with higher frequencies of CRISPR immunity. We conclude that environmental factors that slow down cell growth, rather than the stress caused by bacteriostatic antibiotics, is responsible for increased frequency of CRISPR immunity.

DISCUSSION

Previous studies have identified a number of environmental variables that shape the evolution of CRISPR immunity by affecting the fitness of CRISPR-Cas immune *P. aeruginosa* clones relative to those with mutated phage receptors (Alseth et al., 2019; van Houte et al., 2016; Westra et al., 2015). Here, we identify clinically

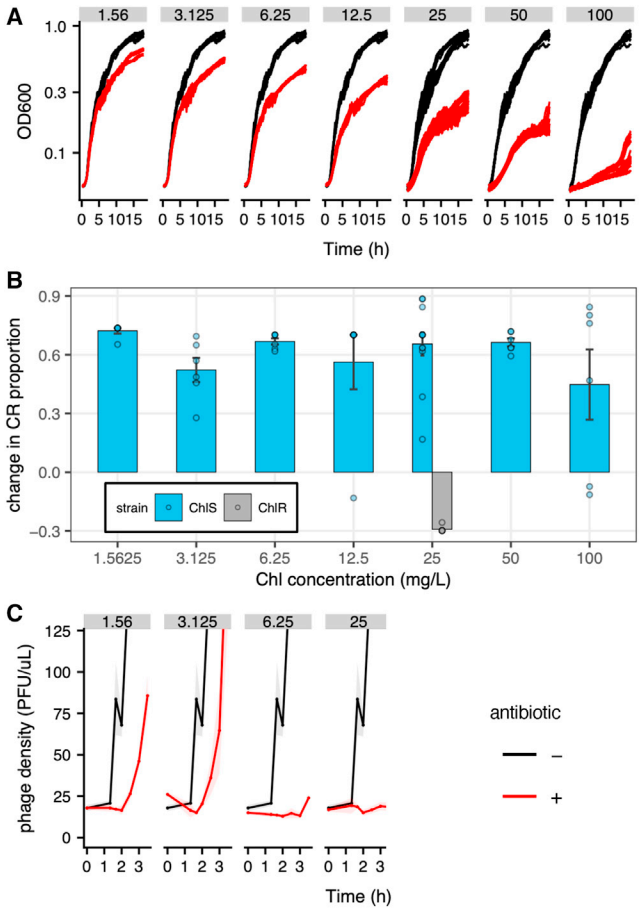

Figure 4. Effect of a large range of Chl concentrations on CRISPR-Cas resistance evolution and phage development dynamics

(A) OD600 growth curves for PA14 grown in the absence (black) or presence (red) of varying Chl doses (μg/mL).

(B) Effect of Chl on the proportion of CRISPR-Cas-resistant clones at 3 d.p.i., compared with the associated no-antibiotic treatment, for PA14 (ChlS) and PA14-*cat* (ChlR). Bars and error bars show mean ± SEM, and individual biological replicates are plotted as dots (n = 6).

(C) One-step phage growth assays in the presence of varying Chl concentrations, after antibiotic pre-exposure for 12 h. The no-antibiotic treatment is shown in black and antibiotic treatments in red, lines and shaded area are, respectively, the mean and SEM (n = 4). See also Figure S7.

relevant environmental factors, which increase the frequency at which sensitive *P. aeruginosa* clones acquire CRISPR immunity during a phage infection. Acquisition of CRISPR immunity depends on the acquisition of spacers from infecting phages, subsequent expression of appropriate protective crRNAs, and interference. Successful acquisition of CRISPR immunity is a major limiting step because cells that just acquired spacers might still be irrevocably damaged before clearing the infection (Horvath and Barrangou, 2010; Jackson et al., 2017; Modell et al., 2017). The factors that determine whether or not bacteria acquire spacers from infecting phages remain unclear. Previously identified determinants of spacer acquisition include the density of defective phages (Hynes et al., 2014), and bacterial nucleases, including crRNA-Cas ribonucleoprotein effector complexes that inactivate the phage and generate DNA breaks and degradation products that serve as substrates for the spacer acquisition machinery (reviewed in Jackson et al. [2017]). Here, we show that the speed of phage development is another key determinant of spacer acquisition by the bacterium, and that bacteriostatic antibiotics promote the acquisition of CRISPR immunity by slowing bacterial growth, which in turn delays phage development. We then extend these results, showing that another parameter controlling growth rates, the carbon source available for bacterial growth, also affects the appearance of CRISPR immunity. Our results suggest that any environmental factors or stresses that slow down cell growth might also promote spacer acquisition, as phage development time is directly linked to bacterial growth rate (Hadas et al., 1997; Jin and Yin, 2021; Rabinovitch et al., 2002).

In some conditions, phage development time might be the main limiting factor for spacer acquisition. For instance, even very low concentrations of Chl had a large effect on phage development dynamics and strongly promoted acquisition of resistance due to CRISPR-Cas, despite having a relatively small effect on exponential growth rate (Figure 4). These data suggest that when cells are growing in optimal conditions, phages may develop too fast for spacer acquisition to be common. Conversely, any stress slowing down cell growth, insofar it also affects phage development time, could in principle increase the probability of spacer acquisition and ultimately cell survival. The CRISPR-Cas system we studied here is already primed against the phage used, favoring primed spacer acquisition. In the absence of priming, slowing down phage growth might be even more crucial for acquisition of spacers that can lead to phage resistance. However, while our data suggest that slower bacterial and phage growth rates will generally favor the evolution of CRISPR immunity, future studies will be needed to experimentally examine how growth rate reductions due to antibiotics and other factors affect primed and naive spacer acquisition in other species with other CRISPR-Cas immune system types.

Interestingly, a number of CRISPR-Cas systems have recently been found to induce dormancy following target recognition (Meeske et al., 2019; Rostøl and Marraffini, 2019; Rostøl et al., 2021) or to be coupled to genes that induce dormancy (Koonin and Zhang, 2017; Makarova et al., 2012). A dormancy response of infected cells with CRISPR immunity can benefit neighboring cells by eliminating phage from the environment and by limiting the invasion of phage mutants that overcome CRISPR immunity (Meeske et al., 2019). Our data suggest a possibility that another advantage of a dormancy response could be that it may lead to more efficient spacer acquisition during infections. In addition, previous studies have shown that targeting early-injected genome sequences of a phage provides more robust levels of CRISPR immunity compared with targeting of late-injected sequences (Modell et al., 2017; Strotskaya et al., 2017) presumably because this offers the CRISPR-Cas system more time to detect and destroy the phage genome. However, competition experiments between CRISPR-immune bacteria and those with SM-based resistance did not show stronger selection for CRISPR-immune bacteria in the presence of bacteriostatic antibiotics, suggesting that they specifically affect the rates of spacer acquisition and not the levels of immunity.

The finding that slower phage development facilitates spacer acquisition may also help to explain why the acquisition of CRISPR immunity is relatively rare under laboratory conditions

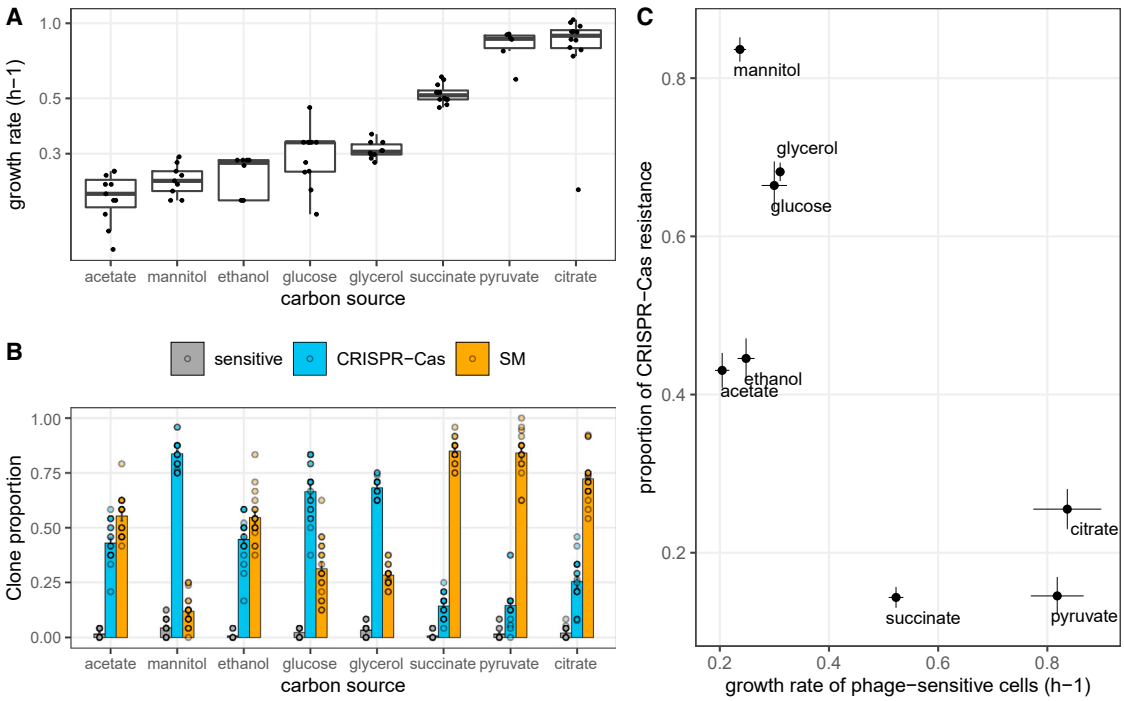

Figure 5. Carbon sources causing slow growth rate also promote CRISPR-Cas evolution

(A) Maximum growth rate from PA14 grown in M9 with different carbon sources. The center value of the boxplots shows the median, boxes the first and third quartile, and individual data points are shown as dots (n= 10).

(B) Proportion of sensitive CRISPR-Cas and SM clones at 4 d.p.i. Bars and error bars show mean ± SEM, and individual biological replicates are plotted as dots (n = 6).

(C) Average bacterial growth rate on each carbon source plotted against the average increase in proportion of CRISPR-Cas immune clones in the evolution experiments, error bars showing SEM.

(Westra and Levin, 2020), in which bacteria commonly grow at rates much higher than in the wild (Gibson et al., 2018) and in clinical contexts. *P. aeruginosa* displays slow growth rates in biofilms (Werner et al., 2004) and in cystic fibrosis (Yang et al., 2008). This will be compounded by exposure to bacteriostatic antibiotics, both in the clinic and in the environment. Promoting CRISPR immunity might have unfortunate consequences, specifically in the context of phage therapy: the rise in antibiotics resistance among bacterial pathogens has caused a resurgence of interest in phage therapy to treat bacterial infections (Kortright et al., 2019). Over the past few years, interest in phage-antibiotic combination therapies has increased in the hope that phage and antibiotics can act in concert to control infections (Kortright et al., 2019; Segall et al., 2019; Tagliaferri et al., 2019; Torres-Barceló and Hochberg, 2016). However, CRISPR-Cas systems are common in *P. aeruginosa* (van Belkum et al., 2015), and *P. aeruginosa* clones that acquire CRISPR immunity can escape these trade-offs and retain virulence (Alseth et al., 2019). Thus, a combination of bacteriostatic antibiotics and phage therapy might steer pathogens toward maintaining both virulence and phage resistance. To consider clinically relevant antibiotic treatments, we asked how PA14 evolves in response to bacteriostatic antibiotics used clinically during treatment of cystic fibrosis infections: sulfamethoxazole, used in combination with Tm, and azithromycin, of particular interest because it reduces virulence even at sub-MIC concentrations (Tateda et al., 2007). Evolution experiments using these antibiotics at sub-inhibitory doses showed a significant increase in the acquisition of CRISPR-Cas immunity with azithromycin and with sulfamethoxazole × Tm treatment (Figure 6). Thus, our results suggest that the choice of antibiotics to use for phage-antibiotic combination therapy should consider the possibility of increased evolution of CRISPR immunity when using bacteriostatic antibiotics, and the potential for pathogenic strains to retain their virulence if they evolve CRISPR-based resistance to phages. Moreover, antibiotics can not only act on non-target bacteria, including other pathogens in multi-species communities but also commensal species. Non-pathogenic commensals will be exposed to antibiotics during antibiotic treatment, potentially more widely promoting CRISPR-Cas immunity in members of the microbiome.

This study specifically examined the effect of antibiotics on the acquisition of CRISPR immunity against phage and demonstrated how bacteriostatic antibiotics can tip the balance in favor of the host immune system by enabling it to launch an immune response before the phage causes irrevocable damage to the host. However, CRISPR-Cas systems can provide defense against a broad range of mobile genetic elements, including plasmids (Marraffini and Sontheimer, 2008), which play a key role in the transmission of antimicrobial resistance (AMR) (Brockhurst et al., 2019). Being able to trigger spacer acquisition from plasmids could therefore have important implications for constraining the spread of AMR genes (Pursey et al., 2018). Recent

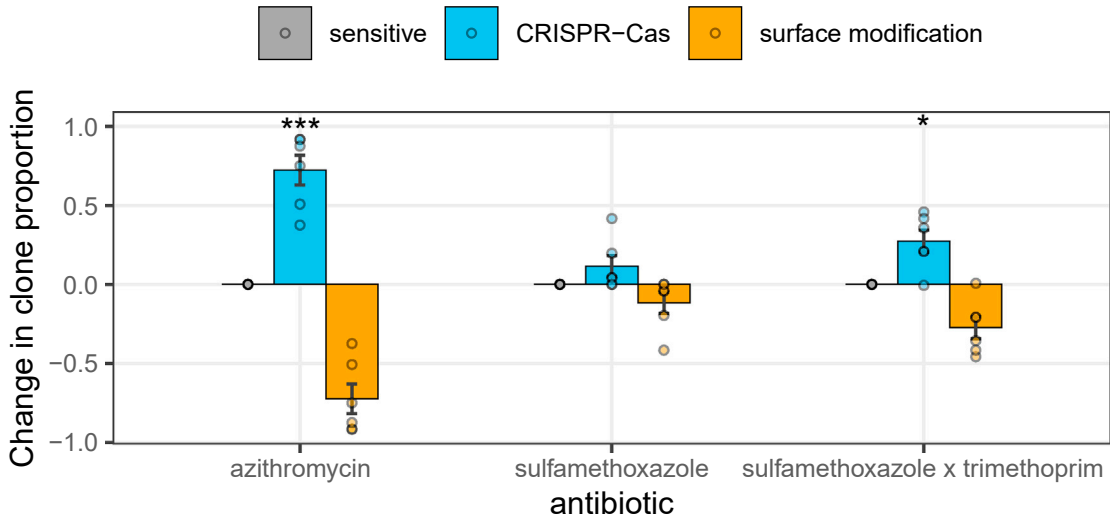

Figure 6. Clinically used antibiotics promote CRISPR-Cas immunity

The effect of antibiotics on the proportion of sensitive (gray), CRISPR-Cas (blue), and SM clones (yellow) is shown at 3 d.p.i., compared with the associated no-antibiotic treatment. Bars and error bars show mean ± SEM, and individual biological replicates are plotted as dots (n = 6). Asterisks indicate antibiotics with CRISPR-Cas proportion significantly different from the associated no-antibiotic treatment (*0.01 < p < 0.05; ***p < 0.001).

studies have demonstrated that the evolution of CRISPR immunity against plasmids can be enhanced using quorum sensing autoinducers, which activate expression of the CRISPR-Cas machinery (Høyland-Kroghsbo et al., 2017; Patterson et al., 2016). Although the precise mechanism remains unclear, evolution of CRISPR immunity against plasmids can also be higher at low temperature or during the late exponential growth phase (Amlinger et al., 2017; Høyland-Kroghsbo et al., 2018). Identifying ways to simultaneously promote spacer acquisition from plasmids and limiting the acquisition of spacers from phage could provide a powerful means to control pathogen abundance, virulence, and their resistance to antibiotics.

STAR★METHODS

Detailed methods are provided in the online version of this paper and include the following:

- KEY RESOURCES TABLE
- RESOURCE AVAILABILITY
  - Lead contact
  - Materials availability
  - Data and code availability
- EXPERIMENTAL MODEL DETAILS
  - Bacterial strains
  - Phages
- METHOD DETAILS
  - Strain and plasmid construction
  - Determination of antibiotic activity
  - Evolution experiments
  - Determination of bacterial growth rate by optical density
  - Determination of bacterial doubling time by microfluidics
  - One-step phage growth assays
  - Determination of antibiotic effects on infection success
  - Measurement of mutation towards SM
  - Spacer acquisition assay
  - Competition assays
  - SOS response assays
  - Cas expression assay
- QUANTIFICATION AND STATISTICAL ANALYSIS

SUPPLEMENTAL INFORMATION

Supplemental information can be found online at https://doi.org/10.1016/j.chom.2021.11.014.

ACKNOWLEDGMENTS

This work was funded by grants from the European Research Council under the European Union's Horizon 2020 research and innovation programme (ERC-2017-ADG-788405 to M.D.S. and ERC-STG-2016-714478 to E.R.W.). E.R.W. was further supported by NERC Independent Research Fellowship (NE/M018350/1). Work in K.S. lab was supported by the Ministry of Science and Higher Education of the Russian Federation under (grant 075-15-2019-1661), NIH National Institute of Health (grant RO1 10407), and the Russian Science Foundation (grant 19-74-20130).

AUTHOR CONTRIBUTIONS

Conceptualization of the study was done by T.D. and E.R.W. Experimental design was carried out by T.D. and E.R.W. Bacterial evolution, competition, and growth experiments, as well as phage infection assays were done by T.D. with assistance from E.K., and MIC measurements were done by E.K. Microfluidics experiments were designed and carried out by U.L. and S.P. Formal analysis of results was done by T.D. K.S. and M.D.S. contributed to discussions and provided feedback throughout the project. T.D. wrote the original draft of the manuscript, with later edits and reviews by T.D., K.S., S.P., M.D.S., and E.R.W.

DECLARATION OF INTERESTS

The authors declare no competing interests.

CellPress
OPEN ACCESS

Received: June 29, 2021
Revised: October 12, 2021
Accepted: November 24, 2021
Published: December 20, 2021

REFERENCES

Alseth, E.O., Pursey, E., Luján, A.M., McLeod, I., Rollie, C., and Westra, E.R. (2019). Bacterial biodiversity drives the evolution of CRISPR-based phage resistance. Nature *574*, 549–552.

Amlinger, L., Hoekzema, M., Wagner, E.G.H., Koskiniemi, S., and Lundgren, M. (2017). Fluorescent CRISPR Adaptation Reporter for rapid quantification of spacer acquisition. Sci. Rep. *7*, 10392.

Baharoglu, Z., and Mazel, D. (2011). *Vibrio cholerae* triggers SOS and mutagenesis in response to a wide range of antibiotics: a route towards multiresistance. Antimicrob. Agents Chemother. *55*, 2438–2441.

Bamford, R.A., Smith, A., Metz, J., Glover, G., Titball, R.W., and Pagliara, S. (2017). Investigating the physiology of viable but non-culturable bacteria by microfluidics and time-lapse microscopy. BMC Biol. *15*, 121.

Barrangou, R., Fremaux, C., Deveau, H., Richards, M., Boyaval, P., Moineau, S., Romero, D.A., and Horvath, P. (2007). CRISPR provides acquired resistance against viruses in prokaryotes. Science *315*, 1709–1712.

Brockhurst, M.A., Harrison, E., Hall, J.P.J., Richards, T., McNally, A., and MacLean, C. (2019). The ecology and evolution of pangenomes. Curr. Biol. *29*, R1094–R1103.

Cady, K.C., Bondy-Denomy, J., Heussler, G.E., Davidson, A.R., and O'Toole, G.A. (2012). The CRISPR/Cas adaptive immune system of *Pseudomonas aeruginosa* mediates resistance to naturally occurring and engineered phages. J. Bacteriol. *194*, 5728–5738.

Cama, J., Voliotis, M., Metz, J., Smith, A., Iannucci, J., Keyser, U.F., Tsaneva-Atanasova, K., and Pagliara, S. (2020). Single-cell microfluidics facilitates the rapid quantification of antibiotic accumulation in Gram-negative bacteria. Lab Chip *20*, 2765–2775.

Chevallereau, A., Meaden, S., van Houte, S., Westra, E.R., and Rollie, C. (2019). The effect of bacterial mutation rate on the evolution of CRISPR-Cas adaptive immunity. Philos. Trans. R. Soc. Lond. B Biol. Sci. *374*, 20180094.

Chevallereau, A., Pons, B.J., van Houte, S., and Westra, E.R. (2021). Interactions between bacterial and phage communities in natural environments. Nat. Rev. Microbiol. https://doi.org/10.1038/s41579-021-00602-y.

Comeau, A.M., Tétart, F., Trojet, S.N., Prère, M.F., and Krisch, H.M. (2007). Phage-antibiotic synergy (PAS): β-lactam and quinolone antibiotics stimulate virulent phage growth. FEMS One *2*, e799.

Datsenko, K.A., Pougach, K., Tikhonov, A., Wanner, B.L., Severinov, K., and Semenova, E. (2012). Molecular memory of prior infections activates the CRISPR/Cas adaptive bacterial immunity system. Nat. Commun. *3*, 945.

Datsenko, K.A., and Wanner, B.L. (2000). One-step inactivation of chromosomal genes in *Escherichia coli* K-12 using PCR products. Proc. Natl. Acad. Sci. USA *97*, 6640–6645.

Dimitriu, T., Szczelkun, M.D., and Westra, E.R. (2020). Evolutionary ecology and interplay of prokaryotic innate and adaptive immune systems. Curr. Biol. *30*, R1189–R1202.

Fineran, P.C., Gerritzen, M.J.H., Suárez-Diez, M., Künne, T., Boekhorst, J., van Hijum, S.A.F.T., Staals, R.H.J., and Brouns, S.J.J. (2014). Degenerate target sites mediate rapid primed CRISPR adaptation. Proc. Natl. Acad. Sci. USA *111*, E1629–E1638.

Gibson, B., Wilson, D.J., Feil, E., and Eyre-Walker, A. (2018). The distribution of bacterial doubling times in the wild. Proc. Biol. Sci. *285*, 20180789.

Hadas, H., Einav, M., Fishov, I., and Zaritsky, A. (1997). Bacteriophage T4 development depends on the physiology of its host *Escherichia coli*. Microbiology (Reading) *143*, 179–185.

Hampton, H.G., Watson, B.N.J., and Fineran, P.C. (2020). The arms race between bacteria and their phage foes. Nature *577*, 327–336.

Horvath, P., and Barrangou, R. (2010). CRISPR/Cas, the immune system of bacteria and archaea. Science *327*, 167–170.

Høyland-Kroghsbo, N.M., Muñoz, K.A., and Bassler, B.L. (2018). Temperature, by controlling growth rate, regulates CRISPR-Cas activity in *Pseudomonas aeruginosa*. mBio *9*, e02184–18.

Høyland-Kroghsbo, N.M., Paczkowski, J., Mukherjee, S., Broniewski, J., Westra, E., Bondy-Denomy, J., and Bassler, B.L. (2017). Quorum sensing controls the *Pseudomonas aeruginosa* CRISPR-Cas adaptive immune system. Proc. Natl. Acad. Sci. USA *114*, 131–135.

Hynes, A.P., Villion, M., and Moineau, S. (2014). Adaptation in bacterial CRISPR-Cas immunity can be driven by defective phages. Nat. Commun. *5*, 4399.

Jackson, S.A., McKenzie, R.E., Fagerlund, R.D., Kieper, S.N., Fineran, P.C., and Brouns, S.J. (2017). CRISPR-Cas: adapting to change. Science *356*, eaal5056.

Jin, T., and Yin, J. (2021). Patterns of virus growth across the diversity of life. Integr. Biol. (Camb) *13*, 44–59.

Kever, L., Hardy, A., Luthe, T., Hünnefeld, M., Gätgens, C., Milke, L., Wiechert, J., Wittmann, J., Moraru, C., Marienhagen, J., and Frunzke, J. (2021). Aminoglycoside antibiotics inhibit phage infection by blocking an early step of the phage infection cycle. bioRxiv. https://doi.org/10.1101/2021.05.02.442312.

Kohanski, M.A., DePristo, M.A., and Collins, J.J. (2010). Sublethal antibiotic treatment leads to multidrug resistance via radical-induced mutagenesis. Mol. Cell *37*, 311–320.

Koonin, E.V., and Zhang, F. (2017). Coupling immunity and programmed cell suicide in prokaryotes: life-or-death choices. Bioessays *39*, 1–9.

Kortright, K.E., Chan, B.K., Koff, J.L., and Turner, P.E. (2019). Phage therapy: a renewed approach to combat antibiotic-resistant bacteria. Cell Host Microbe *25*, 219–232.

Künne, T., Kieper, S.N., Bannenberg, J.W., Vogel, A.I.M., Miellet, W.R., Klein, M., Depken, M., Suarez-Diez, M., and Brouns, S.J.J. (2016). Cas3-derived target DNA degradation fragments fuel primed CRISPR adaptation. Mol. Cell *63*, 852–864.

Labrie, S.J., Samson, J.E., and Moineau, S. (2010). Bacteriophage resistance mechanisms. Nat. Rev. Microbiol. *8*, 317–327.

Langendonk, R.F., Neill, D.R., and Fothergill, J.L. (2021). The building blocks of antimicrobial resistance in *Pseudomonas aeruginosa*: implications for current resistance-breaking therapies. Front. Cell. Infect. Microbiol. *11*, 665759.

Łapińska, U., Glover, G., Capilla-Lasheras, P., Young, A.J., and Pagliara, S. (2019). Bacterial ageing in the absence of external stressors. Philos. Trans. R. Soc. Lond. B Biol. Sci. *374*, 20180442.

Lenski, R.E., Rose, M.R., Simpson, S.C., and Tadler, S.C. (1991). Long-term experimental evolution in *Escherichia coli*. I. Adaptation and divergence during 2,000 generations. Am. Nat. *138*, 1315–1341.

Levy, A., Goren, M.G., Yosef, I., Auster, O., Manor, M., Amitai, G., Edgar, R., Qimron, U., and Sorek, R. (2015). CRISPR adaptation biases explain preference for acquisition of foreign DNA. Nature *520*, 505–510.

Lobritz, M.A., Belenky, P., Porter, C.B.M., Gutierrez, A., Yang, J.H., Schwarz, E.G., Dwyer, D.J., Khalil, A.S., and Collins, J.J. (2015). Antibiotic efficacy is linked to bacterial cellular respiration. Proc. Natl. Acad. Sci. USA *112*, 8173–8180.

Makarova, K.S., Anantharaman, V., Aravind, L., and Koonin, E.V. (2012). Live virus-free or die: coupling of antivirus immunity and programmed suicide or dormancy in prokaryotes. Biol. Direct *7*, 40.

Marraffini, L.A., and Sontheimer, E.J. (2008). CRISPR interference limits horizontal gene transfer in staphylococci by targeting DNA. Science *322*, 1843–1845.

Martínez-García, E., Calles, B., Arévalo-Rodríguez, M., and de Lorenzo, V. (2011). pBAM1: an all-synthetic genetic tool for analysis and construction of complex bacterial phenotypes. BMC Microbiol. *11*, 38.

Meeske, A.J., Nakandakari-Higa, S., and Marraffini, L.A. (2019). Cas13-induced cellular dormancy prevents the rise of CRISPR-resistant bacteriophage. Nature *570*, 241–245.

Modell, J.W., Jiang, W., and Marraffini, L.A. (2017). CRISPR–Cas systems exploit viral DNA injection to establish and maintain adaptive immunity. Nature *544*, 101–104.

Nussenzweig, P.M., McGinn, J., and Marraffini, L.A. (2019). Cas9 cleavage of viral genomes primes the acquisition of new immunological memories. Cell Host Microbe *26*, 515–526.e6.

O'Toole, G.A., and Kolter, R. (1998). Flagellar and twitching motility are necessary for *Pseudomonas aeruginosa* biofilm development. Mol. Microbiol. *30*, 295–304.

Pankey, G.A., and Sabath, L.D. (2004). Clinical relevance of bacteriostatic versus bactericidal mechanisms of action in the treatment of gram-positive bacterial infections. Clin. Infect. Dis. *38*, 864–870.

Patterson, A.G., Jackson, S.A., Taylor, C., Evans, G.B., Salmond, G.P.C., Przybilski, R., Staals, R.H.J., and Fineran, P.C. (2016). Quorum sensing controls adaptive immunity through the regulation of multiple CRISPR-Cas systems. Mol. Cell *64*, 1102–1108.

Payne, P., Geyrhofer, L., Barton, N.H., and Bollback, J.P. (2018). CRISPR-based herd immunity can limit phage epidemics in bacterial populations. eLife *7*, e32035.

Petzoldt, T. (2018). Estimate growth rates from experimental data. R package version 0.7.2. https://github.com/tpetzoldt/growthrates.

Pursey, E., Sünderhauf, D., Gaze, W.H., Westra, E.R., and van Houte, S. (2018). CRISPR-Cas antimicrobials: challenges and future prospects. PLoS Pathog. *14*, e1006990.

Qiu, D., Damron, F.H., Mima, T., Schweizer, H.P., and Yu, H.D. (2008). PBAD-based shuttle vectors for functional analysis of toxic and highly regulated genes in *Pseudomonas* and *Burkholderia spp.* and other bacteria. Appl. Environ. Microbiol. *74*, 7422–7426.

R Core Team (2017). R: A language and environment for statistical computing (R Foundation for Statistical Computing).

Rabinovitch, A., Fishov, I., Hadas, H., Einav, M., and Zaritsky, A. (2002). Bacteriophage T4 development in *Escherichia coli* is growth rate dependent. J. Theor. Biol. *216*, 1–4.

Ramsay, J. (2013). High-throughput β-galactosidase and β-glucuronidase assays using fluorogenic substrates. Bio Protoc. *3*, e827.

Rostøl, J.T., and Marraffini, L.A. (2019). Non-specific degradation of transcripts promotes plasmid clearance during type III-A CRISPR–Cas immunity. Nat. Microbiol. *4*, 656–662.

Rostøl, J.T., Xie, W., Kuryavyi, V., Maguin, P., Kao, K., Froom, R., Patel, D.J., and Marraffini, L.A. (2021). The Card1 nuclease provides defence during type III CRISPR immunity. Nature *590*, 624–629.

Savitskaya, E., Semenova, E., Dedkov, V., Metlitskaya, A., and Severinov, K. (2013). High-throughput analysis of type I-E CRISPR/Cas spacer acquisition in *E. coli*. RNA Biol *10*, 716–725.

Schneider, C.A., Rasband, W.S., and Eliceiri, K.W. (2012). NIH Image to ImageJ: 25 years of image analysis. Nat. Methods *9*, 671–675.

Segall, A.M., Roach, D.R., and Strathdee, S.A. (2019). Stronger together? Perspectives on phage-antibiotic synergy in clinical applications of phage therapy. Curr. Opin. Microbiol. *51*, 46–50.

Severinov, K., Ispolatov, I., and Semenova, E. (2016). The influence of copy-number of targeted extrachromosomal genetic elements on the outcome of CRISPR-Cas defense. Front. Mol. Biosci. *3*, 45.

Shiimori, M., Garrett, S.C., Chambers, D.P., Glover, C.V.C., III, Graveley, B.R., and Terns, M.P. (2017). Role of free DNA ends and protospacer adjacent motifs for CRISPR DNA uptake in *Pyrococcus furiosus*. Nucleic Acids Res. *45*, 11281–11294.

Staals, R.H.J., Jackson, S.A., Biswas, A., Brouns, S.J.J., Brown, C.M., and Fineran, P.C. (2016). Interference-driven spacer acquisition is dominant over naive and primed adaptation in a native CRISPR–Cas system. Nat. Commun. *7*, 12853.

Strotskaya, A., Savitskaya, E., Metlitskaya, A., Morozova, N., Datsenko, K.A., Semenova, E., and Severinov, K. (2017). The action of *Escherichia coli* CRISPR–Cas system on lytic bacteriophages with different lifestyles and development strategies. Nucleic Acids Res. *45*, 1946–1957.

Swarts, D.C., Mosterd, C., van Passel, M.W.J., and Brouns, S.J.J. (2012). CRISPR interference directs strand specific spacer acquisition. PLoS One *7*, e35888.

Tagliaferri, T.L., Jansen, M., and Horz, H.P. (2019). Fighting pathogenic bacteria on two fronts: phages and antibiotics as combined strategy. Front. Cell. Infect. Microbiol. *9*, 22.

Tateda, K., Ishii, Y., Kimura, S., Horikawa, M., Miyairi, S., and Yamaguchi, K. (2007). Suppression of *Pseudomonas aeruginosa* quorum-sensing systems by macrolides: a promising strategy or an oriental mystery? J. Infect. Chemother. *13*, 357–367.

Torres-Barceló, C., Gurney, J., Gougat-Barberá, C., Vasse, M., and Hochberg, M.E. (2018). Transient negative effects of antibiotics on phages do not jeopardise the advantages of combination therapies. FEMS Microbiol. Ecol. *94*, fiy107.

Torres-Barceló, C., and Hochberg, M.E. (2016). Evolutionary rationale for phages as complements of antibiotics. Trends Microbiol. *24*, 249–256.

Torres-Barceló, C., Kojadinovic, M., Moxon, R., and MacLean, R.C. (2015). The SOS response increases bacterial fitness, but not evolvability, under a sublethal dose of antibiotic. Proc. R. Soc. B *282*, 20150885.

Udekwu, K.I., Parrish, N., Ankomah, P., Baquero, F., and Levin, B.R. (2009). Functional relationship between bacterial cell density and the efficacy of antibiotics. J. Antimicrob. Chemother. *63*, 745–757.

van Belkum, A., Soriaga, L.B., LaFave, M.C., Akella, S., Veyrieras, J.B., Barbu, E.M., Shortridge, D., Blanc, B., Hannum, G., Zambardi, G., et al. (2015). Phylogenetic distribution of CRISPR-Cas systems in antibiotic-resistant *Pseudomonas aeruginosa*. mBio *6*, e01796-15.

van Houte, S., Ekroth, A.K.E., Broniewski, J.M., Chabas, H., Ashby, B., Bondy-Denomy, J., Gandon, S., Boots, M., Paterson, S., Buckling, A., and Westra, E.R. (2016). The diversity-generating benefits of a prokaryotic adaptive immune system. Nature *532*, 385–388.

Werner, E., Roe, F., Bugnicourt, A., Franklin, M.J., Heydorn, A., Molin, S., Pitts, B., and Stewart, P.S. (2004). Stratified growth in *Pseudomonas aeruginosa* biofilms. Appl. Environ. Microbiol. *70*, 6188–6196.

Westra, E.R., and Levin, B.R. (2020). It is unclear how important CRISPR-Cas systems are for protecting natural populations of bacteria against infections by mobile genetic elements. Proc. Natl. Acad. Sci. USA *117*, 27777–27785.

Westra, E.R., van Houte, S., Oyesiku-Blakemore, S., Makin, B., Broniewski, J.M., Best, A., Bondy-Denomy, J., Davidson, A., Boots, M., and Buckling, A. (2015). Parasite exposure drives selective evolution of constitutive versus inducible defense. Curr. Biol. *25*, 1043–1049.

Wilke, C.O. (2017). cowplot: Streamlined plot theme and plot annotations for "ggplot2". R package version 0.8.0.

Yang, L., Haagensen, J.A.J., Jelsbak, L., Johansen, H.K., Sternberg, C., Høiby, N., and Molin, S. (2008). In situ growth rates and biofilm development of *Pseudomonas aeruginosa* populations in chronic lung infections. J. Bacteriol. *190*, 2767–2776.

You, L., Suthers, P.F., and Yin, J. (2002). Effects of *Escherichia coli* physiology on growth of phage T7 in vivo and in silico. J. Bacteriol. *184*, 1888–1894.

STAR★METHODS

KEY RESOURCES TABLE

REAGENT or RESOURCE	SOURCE	IDENTIFIER
Bacterial and virus strains		
P. aeruginosa UCBPP-PA14	(Cady et al., 2012)	RefSeq: NC_008463.1
P. aeruginosa UCBPP-PA14 *csy3*::*LacZ*	(Cady et al., 2012)	N/A
P. aeruginosa UCBPP-PA14 BIM-2sp	(Westra et al., 2015)	N/A
P. aeruginosa UCBPP-PA14 *csy3*::*LacZ* surface mutant Sm	(Westra et al., 2015)	N/A
P. aeruginosa UCBPP-PA14 *flgK*::*Tn5B30*(Tc^R)	(O'Toole and Kolter, 1998)	N/A
P. aeruginosa UCBPP-PA14-*cat*(Chl^R)	This study	N/A
E. coli DH5α	Thermo Fisher Scientific	Cat#18265017
DMS3vir	(Cady et al., 2012)	N/A
DMS3vir-acrIF1	(van Houte et al., 2016)	N/A
Chemicals, peptides, and recombinant proteins		
Carbenicillin	Sigma-Aldrich	Cat# C1389
Chloramphenicol	Sigma-Aldrich	Cat# C0378
Ciprofloxacin	Sigma-Aldrich	Cat# 17850
Erythromycin	Sigma-Aldrich	Cat# E5389
Gentamicin sulfate	AppliChem	Cat# A1492
Streptomycin sulfate	Sigma-Aldrich	Cat# S9137
Tetracycline hydrochloride	Sigma-Aldrich	Cat# T7660
Trimethoprim	Sigma-Aldrich	Cat# T7883
Mitomycin C	Abcam	Cat# ab120797
Azithromycin	Sigma-Aldrich	Cat# 75199
Sulfamethoxazole	Sigma-Aldrich	Cat# S7507
Polydimethylsiloxane	Dow Corning	Cat# 184
Deposited data		
Supporting data	This study	Mendeley Data: https://doi.org/10.17632/gbdfwg325y.1
Oligonucleotides		
cat_ins_fwd: TAGATTTAAATGATCGGCACGTAAGAGGTT	IDT	N/A
cat_ins_rev: CTGACCCTTGTCTTACGCCCCGCCCTGCCACT	IDT	N/A
lux_ins_fwd: CTTTTGAAGCTAATTCGATCATGC	IDT	N/A
lux_ins_rev: CATATCAAGCTTAATTCCTTTAATCCCTTTAATTCCTGG	IDT	N/A
Recombinant DNA		
Plasmid pBAM-cat	This study	N/A
Plasmid pHERD30T-pLexA-Lux	This study	N/A
Software and algorithms		
R version 3.4.1	(R Core Team, 2017)	https://cran.r-project.org
R package growthrates	(Petzoldt, 2018)	https://CRAN.R-project.org/package=growthrates
R package cowplot	(Wilke, 2017)	https://CRAN.R-project.org/package=cowplot
ImageJ	(Schneider et al., 2012)	https://imagej.nih.gov/ij/
Labview	National Instruments	https://www.ni.com/en-gb/shop/software/products/labview.html

(*Continued on next page*)

Continued

REAGENT or RESOURCE	SOURCE	IDENTIFIER
MAESFLO	Fluigent	https://www.fluigent.com/product/microfluidic-components-3/software-solutions/
Other		
Synergy 2 Plate reader	Biotek	Cat# 7131000
Varioskan flash plate reader	Thermo Scientific	Cat# N06354
IX73 inverted microscope	Olympus	https://www.olympus-lifescience.com/en/microscopes/inverted/ix73/?gclid=Cj0KCQjwwY-LBhD6ARIsACvT72MKsk2RRA1w8fczQVGZrLT6Cwv8PiGycjAGUhzcmdpgK7aKtkZNBIoaAlDREALw_wcB
UPLSAPO60XW objective	Olympus	Cat# N1480800
Zyla 4.2 sCMOS camera	Andor	https://andor.oxinst.com/products/scmos-camera-series/zyla-4-2-scmos
M-545.USC and P-545.3C7 automated stages	Physik Instrumente	http://www.nanopositioning.net/datasheets/Super-Resolution-Microscope_Stages_with_Capacitive-Feedback.pdf
CoolLED pE300white	Olympus	https://www.coolled.com/products/pe-300white/
MFCS-4C flow control system	Fluigent	https://www.fluigent.com/product/microfluidic-components-3/mfcs-ez-microfluidic-flow-control-system/

RESOURCE AVAILABILITY

Lead contact

Further information and requests for resources and reagents should be directed to and will be fulfilled by the lead contact, Tatiana Dimitriu (t.dimitriu@exeter.ac.uk).

Materials availability

All unique/stable reagents generated in this study are available from the lead contact without restriction.

Data and code availability

Source data are available at Mendeley Data: https://doi.org/10.17632/gbdfwg325y.1.

This paper does not report original code.

Any additional information required to reanalyse the data reported in this paper is available from the lead contact upon request.

EXPERIMENTAL MODEL DETAILS

Bacterial strains

Except when stated otherwise, evolution experiments used *P. aeruginosa* UCBPP-PA14 (PA14) (Cady et al., 2012). UCBPP-PA14 *csy3::lacZ* was used for phage stock amplification, phage titre determination and estimation of Cas protein expression. Competition experiments used a surface mutant (SM) derived from PA14 *csy3::lacZ* and a CRISPR-resistant mutant (BIM-2sp, bacteriophage insensitive mutant with 2 additional acquired spacers against DMS3vir) derived from PA14, both of which have been previously described (Westra et al., 2015). Evolution experiments in the presence of Chl also used PA14-*cat*, a Chl-resistant mutant of PA14 carrying the *cat* gene inserted into the genome. For microfluidics experiments, we used PA14 *flgK::Tn5B30*(Tc^R) (O'Toole and Kolter, 1998).

All bacterial strains were grown at 37 °C in LB broth or M9 medium (22 mM Na_2HPO_4; 22 mM KH_2PO_4; 8.6 mM NaCl; 20 mM NH_4Cl; 1 mM $MgSO_4$; and 0.1 mM $CaCl_2$) supplemented with acetate 20mM, mannitol 40mM, ethanol 40mM, glucose 40mM, glycerol 40mM, succinate 40mM, pyruvate 40mM or citrate 20mM. All liquid cultures were grown with 180 rpm shaking. For experiments using M9 and different carbon sources, overnight pre-cultures were first diluted twice in M9 with the same carbon source.

Phages

Evolution experiments used lytic phage DMS3vir (Cady et al., 2012).DMS3vir and a mutant expressing anti-CRISPR against PA14 IF system, DMS3vir-AcrIF1, were used for determination of resistance phenotypes (van Houte et al., 2016). Phage stocks were obtained from lysates prepared on PA14 *csy3::lacZ* and stored at 4 °C.

METHOD DETAILS

Strain and plasmid construction

PA14-*cat* was constructed by transposon insertion of the *cat* gene into the genome using a variant of plasmid pBAM (Martínez-García et al., 2011) carrying *cat* (pBAM-cat). To this end, the *cat* gene was amplified from plasmid pKD3 (Datsenko and Wanner, 2000) using primers cat_ins_fwd and cat_ins_rev (see key resources table), then ligated into pBAM1 after digestion with SwaI and PshAI.

To measure SOS response expression, the luminescence operon *luxCDABE* under the control of the *lexA* promoter (Torres-Barceló et al., 2015) was amplified by PCR using primers lux_ins_fwd and lux_ins_rev (see key resources table), then ligated into plasmid pHERD30T (Qiu et al., 2008) after digestion with SacI and HindIII, to obtain plasmid pHERD30T-pLexA-Lux.

Determination of antibiotic activity

For MIC (minimum inhibitory concentration) determination, overnight cultures ($\sim$5.10^9 cells /mL) were diluted 10^4-fold in LB medium. 20 μL of the diluted cultures were inoculated into 96-well microplate wells containing 180 μL of LB supplemented with antibiotics using 2-fold serial dilutions of the antibiotic. After 18 h growth at 37 °C, MIC was determined as the lowest antibiotic concentration with no visible growth. To determine the MBC (minimal bactericidal concentration), the content of wells with no visible growth was plated on LB-agar and further incubated overnight. MBC was defined as the lowest antibiotic concentration resulting in 99.9% decrease in initial inoculum cell density (< 5 CFU in 100 μL). MBC/MIC ratio was used to estimate if antibiotic activity was bacteriostatic or bactericidal: a high MBC/MIC ratio indicates that the concentration sufficient to prevent growth is much lower than the concentration required to kill the majority of cells (Pankey and Sabath, 2004). In our assay, antibiotics with average MBC/MIC ratio >1 were the ones that are commonly recognized as being bacteriostatic (Tm, Erm, Chl and Tc).

Evolution experiments

Evolution experiments were performed in glass vials containing 6 mL growth medium and appropriate antibiotics at the concentrations shown in Table S1. Antibiotic concentrations were chosen which were below the MIC and did not affect cell densities after 24h growth too drastically (more than 10-fold) in the absence of phages (as the MIC is not itself a good predictor of antibiotic effect on higher densities of bacteria, (Udekwu et al., 2009)). 60 μL from overnight cultures were co-inoculated with 10^4 plaque-forming units (p.f.u.) of phage DMS3vir, with the exception of the experiment in Figure 5, where a phage inoculum of 10^7 p.f.u. was used. 1:100 volume was then transferred every 24 h into fresh medium for 3 days with the exception of the experiment in Figure 5, which was carried out for 4 days. Each treatment contained 6 biological replicates. Cell densities and phage titers were monitored with serial dilution in M9 salts (after chloroform treatment for phages), and enumeration of colonies on LB-agar and enumeration of plaques on a lawn of PA14 *csy3::lacZ* cells. The identification of phage resistance type (sensitive, CRISPR-Cas or SM) was performed by cross-streaking 24 randomly selected colonies on DMS3vir and DMS3vir-AcrIF1 phages: SM clones are resistant to both phages and have a characteristic smooth colony morphology, whereas clones with CRISPR-Cas immunity are resistant to DMS3vir but sensitive to DMS3vir-AcrIF1 (van Houte et al., 2016).

Determination of bacterial growth rate by optical density

Overnight cultures were diluted 100-fold into fresh growth media. Growth of 200 μL of culture was measured in a 96-well plate by measuring optical density at λ=600nm (OD600) for 14 to 24 h at 37 °C in a BioTek Synergy 2 Plate reader, with 5 s shaking before each measurement. All growth curves were performed in at least 8 replicates. Exponential growth rate in LB was determined in R using the package growthrates (Petzoldt, 2018). For M9 experiments (Figure 5), as growth on some carbon sources did not present one clear exponential growth stage, we first estimated at which stage of growth most phage infections occur in evolution experiments. To this end, we identified for each carbon source the time t_{max}, at which maximal OD was reached in wells inoculated with phages at the same MOI as used in evolution experiments (before OD decreases again when most cells are lysed by phages). The growth rate was then calculated from cultures inoculated without phage, between t_{max} -3h and t_{max}.

Determination of bacterial doubling time by microfluidics

The mother machine device was fabricated and handled as previously reported (Bamford et al., 2017; Cama et al., 2020). Briefly, overnight cultures in LB were spun down via centrifugation for 5 minutes at 4000 rpm at room temperature (Eppendorf 5810 R). The supernatant was filtered twice (Medical Millex-GS Filter, 0.22 μm, Millipore Corp.) and used to re-suspend the bacteria to an OD600 of 75. 2 μl of the bacterial suspension was injected into the microfluidic mother machine device and incubated at 37 °C until there were 1-2 bacteria in the lateral side channels. Fluorinated ethylene propylene tubing (1/32" × 0.008") was connected to the inlet and outlet holes and connected to a computerized pressure-based flow control system (MFCS-4C, Fluigent) controlled by MAESFLO software (Fluigent) and outlet reservoir respectively. Spent media was flushed through the device to wash excess bacteria out of the main channel at 300 μL/h for 8 minutes to completely exchange the fluid in the device and tubing. The chip was mounted on an inverted microscope (IX73 Olympus, Tokyo, Japan) and images were acquired in bright-field via a 60×, 1.2 N.A. objective (UPLSAPO60XW, Olympus) and a sCMOS camera (Zyla 4.2, Andor, Belfast, UK) with a 0.03s exposure. The microfluidic device was moved by two automated stages (M- 545.USC and P-545.3C7, Physik Instrumente, Karlsruhe, Germany, for coarse and fine movements, respectively) to image multiple fields of view in a sequential manner. The imaging setup was controlled by LabView. After acquiring the first set of images, we flowed each of the investigated antibiotics dissolved in LB at the appropriate concentration at 300 μL/h for 8 minutes before

lowering the flow rate to 100 μL/h for 3 hours. The entire assay was carried out at 37 °C in an environmental chamber surrounding the microscope. Bacterial doubling times were extracted from the acquired image sets as previously reported (Łapińska et al., 2019). Briefly, we tracked each individual bacterium and its progeny throughout each experiment and doubling times were measured as the lapses of time between successive bacterial divisions that were assessed by eye through the images loaded in ImageJ (Schneider et al., 2012) and considered to have happened when two daughter cells became clearly distinguishable from their respective parental cell.

One-step phage growth assays

Overnight cultures of PA14 were first diluted into 6 mL growth medium ± antibiotic treatment in glass vials (N=4). For experiments with 30 min of pre-exposure to antibiotics, cells were diluted 25-fold into fresh media with antibiotics and grown for 30 min before phage addition. For experiments with 12 h of pre-exposure to antibiotics, cells were diluted 100-fold into fresh media with antibiotics and grown for 12 h before phage addition. Bactericidal treatments were excluded from further analysis because they caused a 4-fold to 570-fold decrease in cell density after 12 h, making it impossible to determine the latent period of phage under those conditions. After growing in the presence of antibiotics, approximately 5.10^7 p.f.u. of DMS3vir were added in each vial, and vials were vortexed and incubated at 37 °C for 15 min, allowing phage adsorption. Cultures were then diluted 1000-fold into 6 mL growth medium ± antibiotic treatment to limit further adsorption and re-infection, vortexed again and transferred to 24-well plates for parallel processing. Samples were taken immediately (t=0) and then approximately every 20 minutes. The first samples were diluted in M9 salts and plated on LB-agar to quantify cell densities; all samples were chloroform-treated and plated on PA14 *csy3::lacZ* lawns. Phage densities measured after chloroform treatment correspond to the sum of free phages and mature phage particles inside infected cells.

Determination of antibiotic effects on infection success

Four overnight cultures of PA14 were diluted in parallel 100-fold into LB with or without antibiotics. After 2 h growth at 37 °C, DMS3vir phages were added to a final concentration of 1000 p.f.u./mL (equivalent to 5 p.f.u. in the 200 μL total volume in each well) and the vials were vortexed. After 15 min at 37 °C, vials were vortexed again and 24* 200 μL of each individual culture were aliquoted into 24 wells of a 96-well plate. Plates were incubated at 37 °C for 22 h, then 20 μL of each well were spotted on a lawn of PA14 *csy3::lacZ* cells in two replicates. With an average phage inoculum of 5 phages, the distribution of phages across wells is expected to follow a Poisson distribution with 0.7% wells containing 0 phages and 1.3% wells containing more than 10 phages. The control treatment with no antibiotics was consistent with this, as 1 in 96 wells produced no lysis. Lysis indicated that the founding phages reproduced. The number of wells in which phages failed to reproduce was counted for each treatment, and significance was determined by chi-square tests between antibiotic and no-antibiotic treatment.

Measurement of mutation towards SM

To evaluate the frequency of SM cells in the absence of phage selection, cells were grown in LB ± antibiotic treatment for 24 h. After 24 h, cultures were serially diluted in M9 salts, then dilutions were plated both on LB-agar to calculate total cell density, and on LB-agar containing a high concentration of DMS3vir, which was generated by covering the agar surface with a phage stock of 10^8 p.f.u./μL. A pilot experiment confirmed that all colonies growing on top of DMS3vir were phenotypically SM. The density of SM mutants was calculated from counting the number of colonies growing on top of DMS3vir. Three independent experiments were run with 6 experimental replicates each.

Spacer acquisition assay

20 μL of PA14 overnight culture were first diluted 1:50 into 1 mL LB with or without antibiotics in 24-well plates, in 8 replicates per treatment. After 30 min of growth at 37 °C, 2.10^9 DMS3vir phages were added per well, and cultures were incubated at 37 °C for 3h. The density of phage-sensitive cells was measured by plating 100 μL on LB-agar after 10^4-fold dilution in M9 salts. The density of phage-resistant cells was measured by directly plating 100 μL of cultures on LB-agar without dilution: the phage density on these plates was sufficient to prevent growth of sensitive colonies. The majority of colonies had a smooth morphology characteristic of SM clones. We confirmed that smooth colonies were resistant to both DMS3vir and DMS3vir-AcrIF1, whereas non-smooth colonies were resistant to DMS3vir but sensitive to DMS3vir-AcrIF1 and were therefore CRISPR immune. In each culture, the proportion of CRISPR-Cas immune clones within the total population of resistant clones (CRISPR-Cas and SM) was calculated.

Competition assays

Competition experiments were performed in 6 mL LB supplemented in the presence or absence of antibiotics. They were initiated by inoculating 60 μL of a 1:1 mix of LB overnight cultures of CRISPR-Cas immune (BIM-2sp) and surface mutant (SM) clones. For treatments including phages, 8.10^9 p.f.u. DMS3vir were added per vial. Samples were serially diluted at 0 and 24 h and plated on LB agar supplemented with 50 μg/mL 5-bromo-4-chloro-3-indolyl-B-D-galactopyranoside, to determine the ratio of the surface mutant that carries the *LacZ* gene and therefore forms blue colonies, and the BIM-2sp, which forms white colonies. The selection rate of the CRISPR-Cas clone was calculated as m_{BIM2}-m_{3A}, with m the Malthusian parameter defined as $\log(\text{density}(t_1)/\text{density}(t_0))$ (Lenski et al., 1991). We used selection rate rather than relative fitness because some treatments led to an absolute decline in the abundance of the CRISPR-Cas clone.

SOS response assays

To measure SOS response gene expression, pHERD30T-pLexA-Lux was transformed and maintained in PA14 using 50mg/L Gen. To measure SOS expression, PA14 + pHERD30T-pLexA-Lux cells were diluted 100-fold from overnight culture into LB containing the tested antibiotics (and no Gen) and grown for 10h. OD600 and luciferase expression were measured in a BioTek Synergy 2 Plate reader. Standardized luciferase expression was calculated by dividing by OD600 values, after subtracting background measurements of un-inoculated wells.

Cas expression assay

We used PA14 *csy3*::*lacZ* as a reporter strain for Cas gene expression, using the β-Galactosidase fluorogenic substrate 4-Methyl-umbelliferyl β-D-galactoside (Ramsay, 2013) (MUG). An overnight culture of PA14 *csy3*::*lacZ* was diluted 100-fold into 6 mL of LB with or without antibiotics. After 5 h of growth, OD600 was recorded and 100 μL aliquots were immediately frozen at -80 °C. Prior to the assay, the frozen 96-well plate was defrosted and 10 μL were transferred to a new plate and frozen again at -80 °C for 1 h. After transfer to 37 °C, 100 μL reagent solution (0.25 mg/mL MUG and 2 mg/mL lysozyme in phosphate-buffered saline) was added to each well. Fluorescence was measured for 30 min in a Thermo Scientific Varioskan flash plate reader at 37 °C, with excitation and emission wavelengths respectively 365 nm and 450 nm. The 15 min timepoint was used for analysis. Relative fluorescence was calculated as (fluorescence at 15 min – fluorescence at 0 min) / OD600.

QUANTIFICATION AND STATISTICAL ANALYSIS

All statistical analyses were done with R version 3.4.1 (R Core Team, 2017), and package cowplot (Wilke, 2017). Evolution experiments with antibiotics were not all performed simultaneously (Figures 1 and 4): for these, we used individual Student t-tests comparing each treatment to the associated no-antibiotic treatment. For each experiment, statistical parameters are reported in the figure legends or within the results section.